Mutagenesis of the Histidine Ligand in Human Lactoferrin: Iron Binding Properties and Crystal Structure of the Histidine-253 → Methionine Mutant[†,‡]

Hale Nicholson, Bryan F. Anderson, Tony Bland, Steven C. Shewry, John W. Tweedie, and Edward N. Baker*

Department of Biochemistry, Massey University, Palmerston North, New Zealand

Received July 31, 1996; Revised Manuscript Received October 7, 1996[⊗]

ABSTRACT: The contribution of the conserved His ligand to iron binding in transferrins has been addressed by site-directed mutagenesis and X-ray crystallographic analysis. His 253 in the N-terminal half-molecule of human lactoferrin, Lf_N (residues 1−333), has been changed to Gly, Ala, Pro, Thr, Leu, Phe, Met, Tyr, Glu, Gln, and Cys by oligonucleotide-directed mutagenesis. The proteins have been expressed in baby hamster kidney cells, at high levels, and purified. The results show that the His ligand is essential for the stability of the iron binding site. All of the substitutions destabilized iron binding irrespective of whether the replacements were potential iron ligands or not. Iron was lost below pH ∼6 for the Cys, Glu, and Tyr mutants and below pH 7 or higher for the others, compared with pH 5.0 for Lf_N. The destabilization is attributed to both steric and electronic effects. The importance of electronic effects has been shown by the crystal structure of the H253M mutant, which has been determined at an effective resolution of 2.5 Å and refined to a final *R* factor of 0.173. The iron atom is changed from six-coordinate to five-coordinate; the Met 253 side chain is not bound to iron even though there appears to be no steric barrier. This is attributed to the poorer affinity of the thioether ligand for Fe(III) compared with imidazole nitrogen. The decreased stability of the iron binding is attributed solely to the loss of the His ligand as the protein conformation and interdomain interactions are unchanged.

Proteins of the transferrin family, which include serum transferrin and lactoferrin, play a key role in controlling the levels of free iron in the body fluids of animals [for reviews see Brock (1985), Harris and Aisen (1989), and Baker (1994)]. This is achieved through the existence, in each protein, of the two specific binding sites, each with a high affinity for Fe^{3+} iron; binding constants are of the order of 10^{20} M. A general consequence is that the proteins have bacteriostatic properties and also protect against iron-catalyzed free radical formation. In the case of transferrin the bound iron is delivered to cells by receptor-mediated endocytosis (Octave *et al.*, 1983), as a central component of iron metabolism.

The nature of the iron binding sites has been revealed by physicochemical and structural studies (Harris & Aisen, 1989; Baker, 1994). Crystal structures of lactoferrin (Anderson *et al.*, 1987, 1989), transferrin (Bailey *et al.*, 1988), and ovotransferrin (Kurokawa *et al.*, 1995) show that in each case the molecule is folded into two lobes, representing its N- and C-terminal halves, and that each lobe houses a single iron binding site buried deep in a cleft between two protein domains. In each iron binding site the ligands are the same, 1 Asp, 2 Tyr, and 1 His, together with a bound CO_3^{2-} ion. The high affinity of each site for Fe^{3+} must derive both from the perfect fit of the Fe^{3+} and CO_3^{2-} ions when enclosed by the protein and from the choice of ligands. Three anionic oxygen ligands (one carboxylate from Asp, two phenolate from Tyr) match the 3+ charge of the metal ion, and the 2− charge on the CO_3^{2-} is matched by positive charge from an arginine side chain and a helix N-terminus (Figure 1). This gives the overall site a formal net charge close to 0.

Site-directed mutagenesis provides a means to probe the importance of the various ligands that comprise the standard transferrin iron binding site. Mutagenesis of lactoferrin has shown that loss of the Tyr ligands (when replaced by Ala) severely weakens iron binding, although only when *both* Tyr's in a site are removed is binding lost completely (Ward *et al.*, 1996).

Mutagenesis of both lactoferrin (Faber *et al.*, 1996a) and transferrin (Woodworth *et al.*, 1991; Grossmann *et al.*, 1993) demonstrates that replacement of the Asp ligand (by Ser) also weakens iron binding; again this is not sufficient to abolish binding, and the crystal structure of the lactoferrin Asp 60 Ser mutant shows that a water molecule maintains the iron coordination in place of the Asp side chain (Faber *et al.*, 1996a).

The histidine ligand is unusual in that it is the only neutral ligand in the iron coordination sphere. We have chosen to make a series of mutations at this site in order to test the degree to which the His ligand is essential and the consequences of replacing it by a variety of other amino acids. The mutations are made in the context of the N-terminal half-molecule of lactoferrin, Lf_N, which has previously been expressed and characterized (Day *et al.*, 1992a, 1993) and which also has the advantage of the simplicity of a single-sited molecule. Here we describe a number of mutants of

[†] This work was supported in part by the National Institutes of Health (Grant HD-20859), the Wellcome Trust, and the Health Research Council of New Zealand. E.N.B. also received research support as an International Research Scholar of the Howard Hughes Medical Institute.

[‡]The coordinates and structure amplitudes for the H253M crystal structure have been deposited with the Protein Data Bank, Brookhaven, New York, with accession codes 1HSE (coordinates) and R1HSESF (structure amplitudes).

* To whom correspondence should be addressed (air mail). Phone: (64) (6) 350 5367. Fax: (64) (6) 350 5664. Email: T. Baker@massey.ac.nz.

[⊗] Abstract published in *Advance ACS Abstracts,* December 15, 1996.

S0006-2960(96)01908-3 CCC: $14.00

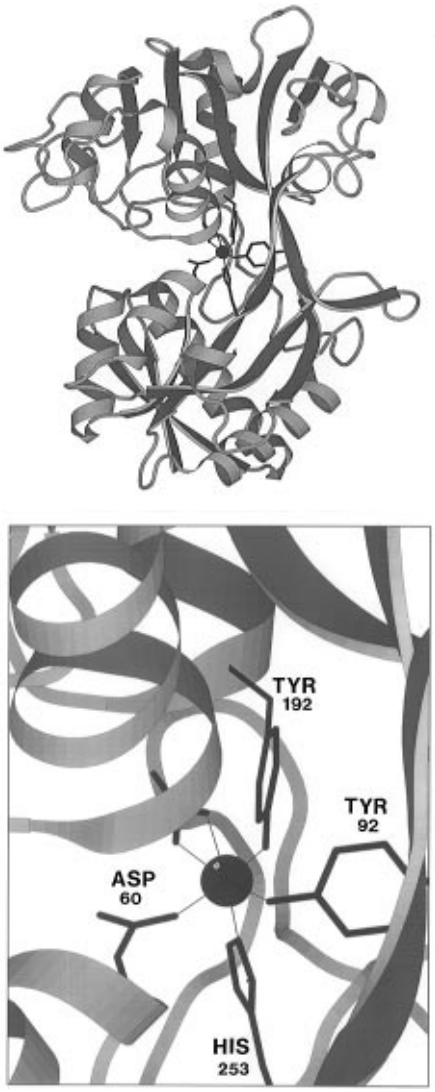

FIGURE 1: (a, top) Schematic representation of the N-terminal half-molecule of human lactoferrin, showing the location of the iron binding site, including His 253. (b, bottom) Close-up view of the ligands that comprise the iron coordination sphere in the N-lobe of lactoferrin.

His 253 and the crystal structure of the His 253 Met (H253M) mutant.

MATERIALS AND METHODS

Mutagenesis. A template for mutagenesis was constructed by inserting the 1314 bp *Sma*I/*Eco*RI fragment encoding residues 250−688 of the human lactoferrin cDNA into the multiple cloning site of M13mp18. Mutations at His 253 were then created by oligonucleotide-directed mutagenesis (Zoller & Smith, 1983), using the *dut*$^-$, *ung*$^-$ procedure to select for the mutant progeny (Kunkel *et al.*, 1987). The mutagenic oligonucleotide chosen was degenerate at the first and second positions of the codon for residue 253 and was either G or C in the third; the sequence NNG/C coded for all possible amino acids at this position. The dioligonucleotide was also designed to ablate the *Bam*HI site in the adjacent multiple cloning site. This allowed an additional selection for the mutant strand by digestion with *Bam*HI following the elongation and ligation reactions.

Putative mutant clones were selected on the basis of the ablated *Bam*HI site. Individual mutants were identified by sequencing the DNA inserts. For each mutant the DNA insert was transferred to the expression vector pNUT (Palmiter *et al.*, 1987) using a modification of the method used previously for the wild-type half-molecule, Lf_N (Day *et al.*, 1992a). The pNUT−Lf_N construct was modified by removal of a 145 bp *Sma*I/*Bgl*II fragment (encoding residues 250−297) and replacement with a 753 bp *Sma*I/*Bgl*II fragment from M13mp18. The modified pNUT−Lf_N vector and the M13 DNA construct containing the required mutation at His 253 were digested with *Sma*I and *Bgl*II. The individual digests were mixed at an appropriate ratio and religated. Following transformation, pNUT−Lf_N clones with the *Sma*I/*Bgl*II insert containing the mutation were identified by examining the size of the fragment released by *Sma*I/*Eco*RI digestion (1.31 versus 1.86 kbp).

Expression and Purification. A subset of the His 253 mutants, covering substitutions of a range of amino acid types, was chosen for large-scale expression and purification. In each case the pNUT−Lf_N mutant plasmid was transfected into baby hamster kidney (BHK) cells as before (Day *et al.*, 1992a; Faber *et al.*, 1996a). Transformed cells were selected with 0.5 mM methotrexate, and expression of the mutant protein from these cells was verified by immunoprecipitation and SDS gel electrophoresis. For large-scale production the cells were transferred into roller bottles. The mutant protein was secreted into the growth medium, which was changed daily (150 mL per day) over a period of 10−14 days. Purification from the spent growth medium was by ion-exchange chromatography (Day *et al.*, 1992a), giving yields in the order of 10−20 mg/L of medium for the various mutants.

Iron Binding. The final pH of the medium from the cell culture was around 5.7−6.0. At this pH some of the mutants were essentially fully saturated with iron (derived from the growth medium), but others were not, some having no iron bound at all. For spectroscopic studies each mutant was therefore dialyzed against 0.05 M Tris-HCl, pH 8.0, containing 0.1 M NaCl, and sufficient 0.01 M ferric nitrilotriacetate solution was added to the protein solution to fully saturate its iron binding capacity. UV−visible spectra in the range 250−820 nm were recorded at room temperature with a Hewlett-Packard HP8452A diode array spectrophotometer.

Iron release as a function of pH was monitored by dialyzing each protein against a series of buffers over the pH range 8.0−2.5 as described previously (Day *et al.*, 1992a). Each solution was maintained for a period of 2 days at the appropriate pH, and the percent saturation with iron was estimated from the visible absorption spectrum, by monitoring the Fe(III)−tyrosine charge transfer band that appears around 450 nm. The precise wavelength of maximum absorption for this band, λ_{max}, varied from one mutant to another and often also varied with pH. For each mutant, the percent saturation with iron at a given pH was therefore estimated by comparing the absorbance at λ_{max} (for that pH) with the absorbance of the fully iron-saturated protein.

Crystallization. Crystallization experiments were undertaken on mutants in their iron-bound form, after first removing their attached carbohydrate chains enzymatically (Baker *et al.*, 1994). This was to ensure homogeneous species. The crystallization conditions were based on those for the wild-type half-molecule (Day *et al.*, 1992b). Concentrated protein solutions (50−70 mg/mL) in 20 μL microdialysis cells (Cambridge Repetition Engineers) were

dialyzed against low ionic strength buffers, pH 7.8−8.2, to which small amounts of alcohol were added.

Crystals were obtained for the Met and Phe mutants, H253M and H253F, under essentially identical conditions, i.e., 0.01 M Tris-HCl, pH 8.0, containing 12% (v/v) 2-propanol. The crystals of H253M were thin square plates, up to 0.3 × 0.3 × 0.05 mm in size, orange-red in color, and heavily overlaid. These proved to be tetragonal, $a = b =$ 58.5 Å and $c = 217.9$ Å, space group $P4_12_12$ (or $P4_32_12$), with one molecule in the asymmetric unit. Based on an assumed molecular mass of 37.5 kDa these had a Matthews coefficient (Matthews, 1968) of $V_M = 2.49$ Å^3/Da and a solvent content of 51%. The crystals of H253F were quite different, i.e., colorless needles, 0.2 × 0.03 × 0.03 mm in size. Although too small for X-ray analysis, they appeared to have a trigonal or hexagonal unit cell with approximate dimensions $a = b = 151.0$ Å, $c = 48.5$ Å, $\alpha = \beta = 90°$, and $\gamma = 120°$.

Data Collection. A crystal of the H253M mutant, 0.3 × 0.2 × 0.04 mm in size, carefully cut from a cluster, was used for data collection on an R-Axis IIC image plate detector, using radiation from a Rigaku RU200 rotating anode generator (Cu Kα, $\lambda = 1.5418$ Å). Data were collected at room temperature, with the crystal mounted approximately about its unique [*c*] axis but offset by about 10°. The length of the [*c*] axis required that a relatively long crystal-to-detector distance be used. The result was that the data were essentially complete to 2.5 Å resolution but that higher resolution data were limited to the corners of the image plate. Thus, although the nominal maximum resolution of the data was 2.2 Å, and the high-resolution data contributed to the refinement and the precision of the refined structure, the effective resolution may be closer to 2.5 Å. (Note that the offset of the crystal from a crystal axis helped ensure that the missing high-resolution data were reasonably evenly distributed through reciprocal space.)

Data were processed using the supplied R-Axis software (Molecular Structure Corp.). From a total of 40 996 measurements with $I > 1.0\sigma_I$, 14 575 unique reflections to a maximum resolution of 2.2 Å were obtained. This represented a data set that was 90% complete to 2.5 Å and 72% complete to 2.2 Å (42% complete in the outer 2.5−2.2 Å shell). The overall merging *R* for redundant measurements was 0.066, with a multiplicity of 2.8 (merging *R* 0.215 and multiplicity 1.8 in the outer shell). Data collection statistics are summarized in Table 1.

Structure Determination and Refinement. The H253M crystals were isomorphous with a tetragonal crystal form originally obtained for the wild-type half-molecule (Day *et al.*, 1992b). The latter was originally assumed to be a metal-free form of the protein, but subsequent crystallographic analysis (Day, 1993) showed that this was not the case; the conformation was "closed", very similar to that of the iron-bound form of Lf_N, with an unidentified species present in the metal binding site.

An initial model for the H253M mutant was obtained from the tetragonal wild-type structure, described above. This had been solved by molecular replacement, shown to be in space group $P4_12_12$ rather than $P4_32_13$, and refined by restrained least squares to an *R* factor of 0.211 for all data to 2.3 Å resolution (Day, 1993). To construct the initial model for H253M, all solvent molecules and ions, and the side chains of Asp 60, Tyr 92, Arg 121, Tyr 192, and His 253 (the binding site ligands) were removed. The space group was also assumed to be $P4_12_12$, as for the wild-type structure.

Table 1: H253M Data Collection, Refinement, and Model Statistics

data collection	
max resolution (Å)	2.2
no. of observations	40996
no. of unique reflections	14575
completeness of data (%), overall (2.5−2.2 Å)	74 (42)
multiplicity, overall (2.5−2.2 Å)	2.8 (1.8)
R_{merge}, overall (2.5−2.2 Å)	0.101 (0.215)
final refinement and model parameters	
resolution range (Å)	20−2.2
no. of reflections	14537
no. of protein atoms	2405
no. of ions	$1Fe^{3+}$, $1CO_3^{2-}$
no. of solvent molecules	113
R factor	0.173
av *B* factor (protein) (Å^2)	31.2
av *B* factor (solvent) (Å^2)	48.0
rmsd of protein geometry from std values	
bond lengths (Å)	0.016
bond angles (deg)	1.6
planes (Å)	0.015

Least squares refinement of the structure was with TNT (Tronrud *et al.*, 1987). The starting model was subjected first to several rounds of rigid body refinement in which the molecule was treated initially as a single rigid body and then as two separate domains. This reduced the *R* factor to 0.312 for data in the resolution range 20.0−5.0 Å. Further refinement was by restrained least squares, using TNT with the geometry library of Engh and Huber (1991). A $2F_o - F_c$ electron density map calculated at the start of refinement showed little or no density for residues 1−4 or for residues beyond 311, and the starting model therefore comprised residues 5−311 only. Electron density became visible for residues 312−321 later in the refinement, allowing these to be fitted. Refinement proceeded in a series of rounds of restrained least squares refinement, of 20−30 cycles each, interspersed with model examination and rebuilding on a graphics workstation using FRODO (Jones, 1978). Both $2F_o - F_c$ and $F_o - F_c$ electron density maps were used for model rebuilding. The side chains of Met 253, Asp 60, Tyr 92, Arg 121, and Tyr 192, together with the Fe^{3+} and CO_3^{2-} ions, were all built into the model when the *R* factor was ∼0.28 and were also checked with omit maps later in refinement. *B* values were all set at 25 Å^2 at the start of refinement but were allowed to assume individual isotropic values from $R = 0.28$ onward. No restraints were placed on the Fe−ligand bond lengths or angles. No solvent molecules were included in the model until the *R* factor reached 0.21, and they were then introduced conservatively; solvent molecules were not included unless electron density was present in both $2F_o - F_c$ and $F_o - F_c$ maps (levels 1.00 and 3.00) and they made reasonable geometrical contact with potential partners. All were assumed to be water. The standard bulk solvent model incorporated in TNT (Tronrud *et al.*, 1987) was used throughout the refinement.

The final model, comprising 2405 protein atoms (residues 5−321), 1 Fe^{3+} and 1 CO_3^{2-} ion, and 113 water molecules, gave an *R* factor of 0.173 for all data in the resolution range 20.0−2.2 Å (14 537 reflections). The rms deviations from standard bond lengths and angles are 0.016 Å and 1.6°, respectively; other refinement details are in Table 1. In the Ramachandran plot calculated from the final model, 85%

Table 2: Iron Binding and Release by Mutants

protein	λ_{max} (nm)	iron release[a]	pH_{50}[b]
wild type	452	5.0−4.0	4.4
H253E	444	6.2−5.0	5.8
H253C	446	6.1−5.4	5.7
H253M	430	7.0−6.0	6.6
H253L	420	nd	nd
H253T	426	nd	nd
H253F	430	7.0−6.0	6.7
H253Y	424	6.5−5.5	6.1
H253Q	428	>7.1	nd
H253A	436	nd	nd
H253G	430	>7.1	nd
H253P	424	>7.1	nd

[a] pH range over which iron is released. nd = not determined. [b] pH at which 50% of iron is released.

of residues are in the most favorable (ϕ, φ) regions, as defined in the program PROCHECK (Laskowski *et al.*, 1993). As in the other lactoferrin half-molecule structures, the only outlier is Leu 299, which is the central residue in a classic γ-turn, and has standard values of around (70, −50°) (Baker & Hubbard, 1984).

RESULTS AND DISCUSSION

Iron Binding. All of the mutants bound iron at pH 8.0 and gave electronic spectra that were broadly similar to the wild-type half-molecule. The visible spectrum is characterized by an absorption peak at a wavelength around 450 nm; this peak arises from a ligand-to-metal charge transfer (LMCT) transition, assigned as phenolate $\pi \rightarrow$ d (Fe^{3+}) (Gaber *et al.*, 1974); i.e., it reflects the Fe(III)−Tyr interaction. The values of λ_{max} for the mutants are all lower than for wild-type Lf_N (Table 2). Only for the Cys and Glu mutants, H253C and H253E, is λ_{max} close to that of wild type; for all the others it is in the range 420−436 nm, similar to the value for the D60S mutant (434 nm) in which a water molecule replaces the Asp ligand (Faber *et al.*, 1996a).

The stability of iron binding is also markedly affected by mutation of His 253, with all of the mutants being significantly less stable to acidic pH than wild-type Lf_N. The closest to wild type is the Cys mutant which begins to lose iron at a pH around 6.1, compared with 5.0 for Lf_N under the conditions of our experiment, followed by the Glu and Tyr mutants for which iron release begins at pH values of approximately 6.3 and 6.5, respectively. These three mutants are all species in which the substituted amino acid has the potential to act as an iron ligand. All of the remaining mutants have significantly lower iron stability; these include some for which the substituted amino acid *cannot* bind to iron (Leu, Phe, Ala, Gly, Pro) but others (Met and Gln) in which it might be predicted to act as a ligand. Typical iron release profiles for some of these mutants are shown in Figure 2.

The data suggest that for the Cys and Glu mutants, and possibly also Tyr, the substituted amino acid may act as an iron ligand. Modeling these substitutions on the Lf_N structure suggests, however, that neither Cys nor Tyr side chains could coordinate to iron without some adjustment of the structure. A Cys side chain is too short for Sγ to approach closer than 3.4 Å from the iron atom without displacement of the polypeptide chain (i.e., small adjustments of the torsion angles are not sufficient). On the other hand, a Tyr side chain is too large to fit without significant adjustments. This

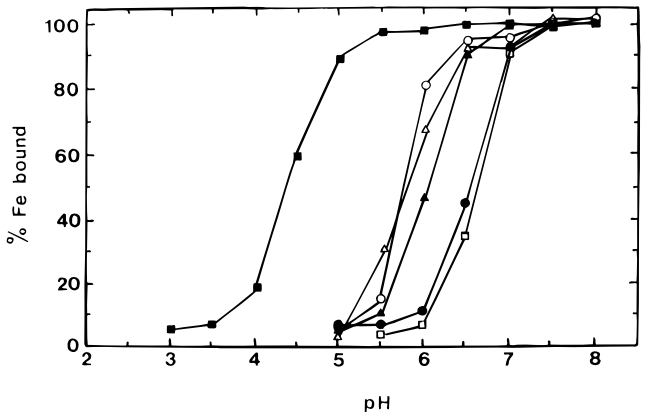

FIGURE 2: Plots showing pH dependence of iron release from lactoferrin mutants in which His 253 is replaced by Cys (○), Glu (△), Tyr (▲), Met (●), and Phe (□) compared with wild-type Lf_N (■).

steric misfitting may explain the lower stability of these two mutants. The decreased stability of iron binding of the H253Y mutant mirrors observations made with transferrin, for which the analogous H249Y mutant shows much more rapid iron release than wild type (Zak *et al.*, 1995). In the case of the Glu mutant the carboxyl group could coordinate without any significant structural adjustment; here the lower stability may result from the added negative charge when an anionic ligand (Glu) replaces the neutral His.

All of the other mutants show a similar pattern of reduced stability and λ_{max} in the range 420−436 nm. This suggests that the low value of λ_{max} may be diagnostic of the loss of a protein ligand, as occurs in the D60S mutant (Faber *et al.*, 1996). It was for this reason that two mutants from the latter group, H253M and H253F, were chosen for crystallization trials; the H253M mutant was of particular interest because Met is a potential iron ligand, and modeling on Lf_N indicated that its thioether sulfur should be able to approach to at least 2.2 Å from the iron atom (see below), yet it groups with the noncoordinating mutants.

Structure of H253M. The overall protein conformation of the H253M mutant is unchanged from that of wild-type Lf_N. Superposition of the C_α atoms of residues 5−310, i.e., the whole molecule apart from a small number of residues at the N- and C-termini, gives an overall rms deviation of 0.31 Å. This implies that even the relative orientations of the two domains are the same as in Lf_N. It reflects the fact that His 253 does not contribute to interdomain interactions, and its substitution by Met does not signficantly perturb the interdomain region (see below).

The close similarity of the domain orientations in the H253M mutant and in wild-type Lf_N appears to be a molecular property and not a result of crystal packing interactions. This is seen by comparing these two species with other Lf_N mutants, D60S (Faber *et al.*, 1996a) and R121S and R121E (Faber *et al.*, 1996b). In all these crystal structures the crystal packing contacts involve the same residues, i.e., Arg 27, Arg 28, Arg 30, and Ser 283 on domain 1 and Glu 178, Asn 179, Asp 205, and Asp 220 on domain 2. In spite of this, relative domain orientations can vary considerably, with differences 3.5−7.5° from those in Lf_N and H253M. The combination of altered domain orientations with conserved intermolecular contacts results in different crystal unit cells. Most striking is the comparison of H253M with D60S. All of the crystal contacts less than 3.3 Å found

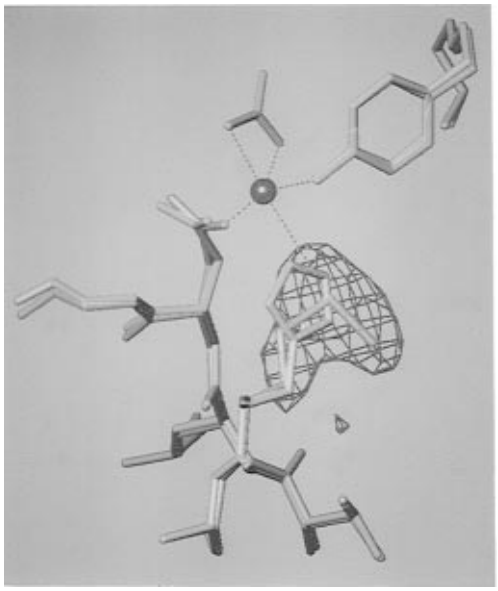

FIGURE 3: Superposition of the iron site of the H253M mutant (blue) onto wild-type Lf_N (yellow), showing also the difference electron density for the Met side chain (at a contour level of 5σ). Figure prepared with TURBO FRODO (Roussel & Cambillau, 1991).

for H253M are also found for D60S, but the two domains in D60S are 7.5° more closed and the unit cell is changed from space group $P4_12_12$ (H253M) to $C2$ (D60S).

As in the other half-molecule structures, the C-terminus is disordered. In Lf_N, residues 323−327 are in an extended conformation, and no density can be seen for residues 328−333; in R121S and R121E no density can be seen beyond Phe 325, and here interpretable density does not continue beyond Gly 321.

At the mutation site the most important observation is that the Met side chain is *not* coordinated to the metal ion; i.e., the iron is five-coordinate rather than six-coordinate. This undoubtedly explains the weakened iron binding and explains why the Met mutant behaves like the other mutants with noncoordinating side chains in place of His, i.e., H253G, H253A, H253P, and H253F. The methionine side chain is extended with torsion angles $\chi_1 = -75.0°$ and $\chi_2 = 171.0°$, which places the S_δ atom 3.68 Å from the metal, too far for even a weak interaction. This seems surprising, since only small adjustments are required to bring the S_δ atom within bonding distance of the iron atom. A change of the main chain torsion angles (ϕ, φ) from (−68°, 155°) to (−74°, 158°) and of the side chain torsion angles (χ_1, χ_2) from (−75°, 171°) to (−71°, 166°) would make the Fe−S_δ(253) distance 2.2 Å and introduce no serious steric clashes (all contacts >3.2 Å). The electron density makes it clear, however (Figure 3), that the Met side chain is not coordinated and the iron is five-coordinate. The other Fe−ligand distances, and hydrogen bonds involving the anion, are unchanged from those in the wild-type Lf_N, within the estimated experimental error of around 0.1−0.15Å (Table 3). Superposition of all the atoms of the binding site except Met 253, i.e., Asp 60, Tyr 92, Thr 117, residues 121−124, and Tyr 192, Fe^{3+} and CO_3^{2-} (71 atoms), onto the equivalent atoms of Lf_N gives an rms deviation of only 0.25 Å.

Table 3: Distances in the Metal and Anion Sites (Å)

	metal−ligand distances			hydrogen bond distances	
	H253M	Lf_N		H253M	Lf_N
Fe−$O_{\delta1}$ (60)	1.99	1.99	O1···N_ϵ (121)	3.02	2.90
Fe−O_η (92)	2.10	2.00	O1···$N_{\eta2}$ (121)	2.92	2.59
Fe−O_η (192)	1.86	1.92	O2···N (123)	2.75	2.81
Fe−S_δ (253)	(3.68)	2.15[a]	O3···$O_{\gamma1}$ (117)	2.66	2.64
Fe−O1[b]	2.12	2.09	O3···N (124)	3.02	3.31
Fe−O2[b]	2.19	2.23			

[a] To His 253 $N_{\epsilon2}$. [b] Carbonate oxygen atoms.

The methionine side chain occupies slightly more space than histidine, but this does not disturb any of the other residues close to it in the interdomain space; Glu 81, Tyr 82, Tyr 92, Tyr 192, Arg 210, Glu 216, and Lys 301 all superimpose closely (rms deviation 0.32 Å), as shown in Figure 4, and the only change is a displacement of the water molecule previously attached to $N_{\delta1}$ of His 253. Interdomain interactions which help stabilize the closed state are unchanged from those in Lf_N, implying that it is only the loss of the His ligand that destabilizes the iron binding ability of the mutant.

The final model contains 113 solvent molecules, all regarded as water. More than half of these (59) superimpose to within 1.0 Å of solvent molecules located independently in the structure of the wild-type molecule. Of 15 essentially

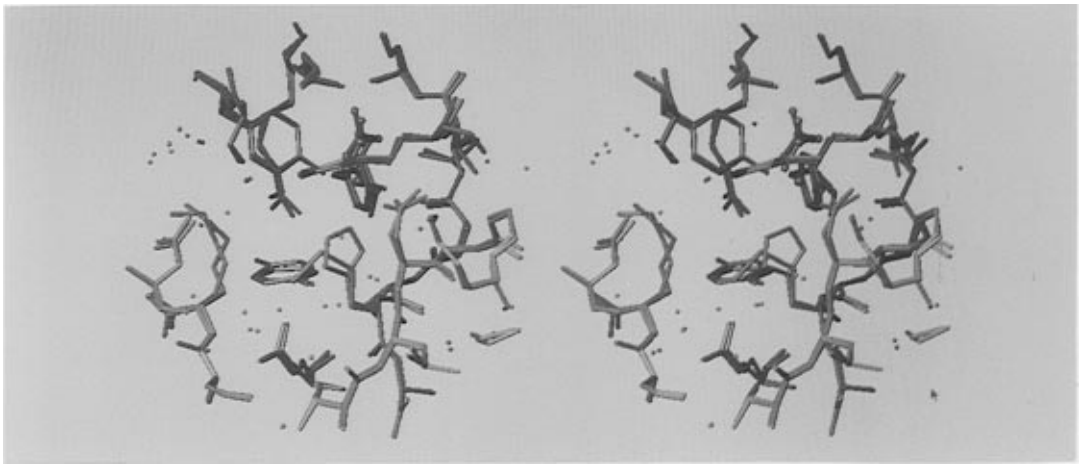

FIGURE 4: Stereo diagram showing surrounds of residue 253 in the interdomain region of the H253M mutant (pink), compared with wild-type Lf_N (blue). Residues from domain 2 are shown in darker colors at the top of the picture and residues from domain 1 in lighter colors at the bottom. The iron atom is shown with a larger sphere. Both domains show very close correspondence, with only some disturbance in water molecule positions immediately adjacent to the mutation site. Figure prepared with TURBO FRODO (Roussel & Cambillau, 1991).

discrete internal water molecules found in the latter, all but one are present in H253M, the one that is missing being the water molecule displaced when His 253 is replaced by Met. The water molecules in the large cavity of the interdomain cleft are much less well conserved, however; only 7 out of 16 from Lf_N are retained within 1.5 Å. These have fewer protein ligands and higher *B* values, reinforcing the view that the water in this cavity is not well ordered except where it is tied down by protein groups. These latter water molecules do not contribute much to interdomain interactions.

OVERALL CONCLUSIONS

The results show that the neutral His ligand does contribute materially to the stability of iron binding in lactoferrin and presumably also in other transferrins. When it is replaced by other potential iron ligands such as Glu, Cys, Tyr, and Met, these substitutions are significantly destabilizing. It seems that although iron binding involves a structural transition from an "open" to a "closed" form, and might therefore be expected to show some flexibility, the "closed" state is in fact quite restrictive. The invariance of the His ligand in transferrin iron sites probably reflects both electronic and steric factors. Substitution by Glu is sterically acceptable but appears to be electronically unfavorable (by adding an additional, uncompensated, negative charge in the binding site). Substitution by Met is also sterically acceptable (shown by the identical domain closure of the H253M mutant), but it is an inappropriate ligand (see below). On the other hand, substitution by Cys or Tyr must also introduce some steric problems; modeling suggests that neither can coordinate to iron without some adjustment of the polypeptide chain. Even complete loss of the ligand, however, leaving a five-coordinate iron, as in H253M, does not abolish iron binding at pH values greater than 7, nor does it signficantly change the iron geometry with respect to the other ligands or the domain closure. At first sight it might seem surprising that the Met ligand does not bind to iron in this mutant, when there does not seem to be any steric barrier, but this presumably reflects the lower affinity for the neutral thioether group compared with anionic oxygen ligands or the strong σ donor nitrogen of histidine. Methionine is known to be a ligand to the low-spin iron of *c*-type cytochromes (Mathews, 1985) but is probably a much poorer ligand for the high-spin Fe(III) of transferrins.

REFERENCES

Anderson, B. F., Baker, H. M., Dodson, E. J., Norris, G. E., Rumball, S. V., Waters, J. M., & Baker, E. N. (1987) *Proc. Natl. Acad. Sci. U.S.A. 84*, 1769−1773.

Anderson, B. F., Baker, H. M., Norris, G. E., Rice, D. W., & Baker, E. N. (1989) *J. Mol. Biol. 209*, 711−734.

Bailey, S., Evans, R. W., Garratt, R. C., Gorinsky, B., Hasnain, S., Horsburgh, C., Jhoti, H., Lindley, P. F., Mydin, A., Sarra, R., & Watson, J. L. (1988) *Biochemistry 27*, 5804−5812.

Baker, E. N. (1994) *Adv. Inorg. Chem. 41*, 380−463.

Baker, E. N., & Hubbard, R. E. (1984) *Prog. Biophys. Mol. Biol. 44*, 97−179.

Baker, H. M., Day, C. L., Norris, G. E., & Baker, E. N. (1994) *Acta Crystallogr., Sect. D 50*, 380−384.

Brock, J. H. (1985) in *Metalloproteins* (Harrison, P., Ed.) Part 2, pp 183−262, Macmillan Press, London.

Day, C. L. (1993) Ph.D. Thesis, Massey University, New Zealand.

Day, C. L., Stowell, K. M., Baker, E. N., & Tweedie, J. W. (1992a) *J. Biol. Chem. 267*, 13857−13862.

Day, C. L., Norris, G. E., Anderson, B. F., Tweedie, J. W., & Baker, E. N. (1992b) *J. Mol. Biol. 228*, 973−974.

Day, C. L., Anderson, B. F., Tweedie, J. W., & Baker, E. N. (1993) *J. Mol. Biol. 232*, 1084−1100.

Engh, R. A., & Huber, R. (1991) *Acta Crystallogr., Sect. A 47*, 392−400.

Faber, H. R., Bland, T., Day, C. L., Norris, G. E., Tweedie, J. W., & Baker, E. N. (1996a) *J. Mol. Biol. 256*, 352−363.

Faber, H. R., Baker, C. J., Day, C. L., Tweedie, J. W., & Baker, E. N. (1996b) *Biochemistry* (in press).

Gaber, B. P., Miskowski, V., & Spiro, T. G. (1974) *J. Am. Chem. Soc. 96*, 6868−6873.

Grossmann, J. G., Mason, A. B., Woodworth, R. C., Neu, M., Lindley, P. F., & Hasnain, S. S. (1993) *J. Mol. Biol. 231*, 554−558.

Harris, D. C., & Aisen, P. (1989) in *Iron Carriers and Iron Proteins* (Loehr, T. M., Ed.) pp 241−351, VCH Publishers, New York.

Jones, T. A. (1978) *J. Appl. Crystallogr. 11*, 268−272.

Kunkel, T. A., Roberts, J. D., & Zakour, R. A. (1987) *Methods Enzymol. 154*, 367−382.

Kurokawa, J., Mikami, B., & Hirose, M. (1995) *J. Mol. Biol. 254*, 196−207.

Laskowski, R. A., MacArthur, M. W., Moss, D. S., & Thornton, J. M. (1993) *J. Appl. Crystallogr. 26*, 283−291.

Luzzati, V. (1952) *Acta Crystallogr. 5*, 802−810.

Mathews, F. S. (1985) *Prog. Biophys. Mol. Biol. 45*, 1−56.

Matthews, B. W. (1968) *J. Mol. Biol. 33*, 491−497.

Octave, J.-N., Schneider, Y.-J., Trouet, A., & Crichton, R. R. (1983) *Trends Biochem. Sci. 8*, 217−220.

Palmiter, R. D., Behringer, R. R., Quaife, C. J., Maxwell, F., Maxwell, I. H., & Brinster, R. L. (1987) *Cell 50*, 435−443.

Ramakrishnan, C., & Ramachandran, G. N. (1965) *Biophys. J. 5*, 909−933.

Read, R. J. (1986) *Acta Crystallogr., Sect. A 42*, 140−149.

Roussel, A., & Cambillau, C. (1991) *TURBO FRODO, Silicon Graphics Geometry Partners Directory* (Silicon Graphics, Ed.) p 86, Silicon Graphics, Mountain View, CA.

Tronrud, D. E., Ten Eyck, L. F., & Matthews, B. W. (1987) *Acta Crystallogr., Sect. A 43*, 489−501.

Ward, P. P., Zhou, X., & Conneely, O. M. (1996) *J. Biol. Chem. 271*, 12790−12794.

Woodworth, R. C., Mason, A. B., Funk, W. D., & MacGillivray, R. T. A. (1991) *Biochemistry 30*, 10824−10829.

Zak, O., Aisen, P., Crawley, J. B., Joannou, C. L., Patel, K. J., Rafiq, M., & Evans, R. W. (1995) *Biochemistry 34*, 14428−14434.

Zoller, M. J., & Smith, M. (1983) *Methods Enzymol. 100*, 468−500.

BI961908Y